

Review

## Recent Advances in the LiFeO<sub>2</sub>-based Materials for Li-ion Batteries

Jiangang Li<sup>1</sup>, Jianjun Li<sup>2</sup>, Jing Luo<sup>1</sup>, Li Wang<sup>2</sup>, Xiangming He<sup>2,\*</sup>

<sup>1</sup> Department of Applied Chemistry, Beijing Institute of Petrochemical Technology, Beijing 102617

<sup>2</sup> Institute of Nuclear and New Energy Technology, Tsinghua University, Beijing 100084, China

\*E-mail: [hexm@tsinghua.edu.cn](mailto:hexm@tsinghua.edu.cn)

Received: 19 December 2010 / Accepted: 20 January 2011 / Published: 1 May 2011

---

LiCoO<sub>2</sub> has been the most widely used cathode material in commercial Li-ion batteries. Nevertheless, cobalt has economic and environmental problems that leave the door open to exploit alternative cathode materials, among which, LiFeO<sub>2</sub> with similar rock-salt structure to LiCoO<sub>2</sub>, has been paid more attention due to most abundance and non-toxicity of Fe. Recent advances in LiFeO<sub>2</sub>-based cathode materials are summarized in this paper. The preparation and the performance are reviewed, and the future LiFeO<sub>2</sub>-based promising cathode materials are also prospected.

---

**Keywords:** Li-ion batteries, LiFeO<sub>2</sub>-based materials, review

### 1. INTRODUCTION

Ordered rock-salt  $\alpha$ -NaFeO<sub>2</sub>-type LiMO<sub>2</sub> (M: Co, Ni<sub>1-x-y</sub>Mn<sub>x</sub>Co<sub>y</sub> etc.) cathode materials have been widely used in commercial Li-ion batteries due to better electrochemical performance. Nevertheless, cobalt and nickel has economic and environmental problems that limit its use in large-scale Li-ion batteries for EV and electric storage station. Therefore alternative cathode materials with low cost and non-toxicity have been studied in recent years. LiFeO<sub>2</sub>, with similar rock-salt structure to LiCoO<sub>2</sub>, has been paid more attention due to most abundance and non-toxicity of Fe. Great progress have been made recently on its preparation, structure and modification due to extensive use of new preparation methods such as hydrothermal, low-temperature solid state reaction etc., and new analysis instruments such as Mössbauer spectra, HRTEM etc.. Recent advances in LiFeO<sub>2</sub>-based cathode materials are summarized in this paper. The preparation and the performance are reviewed, and the future LiFeO<sub>2</sub>-based promising cathode materials are also prospected.

## 2. LiFeO<sub>2</sub>

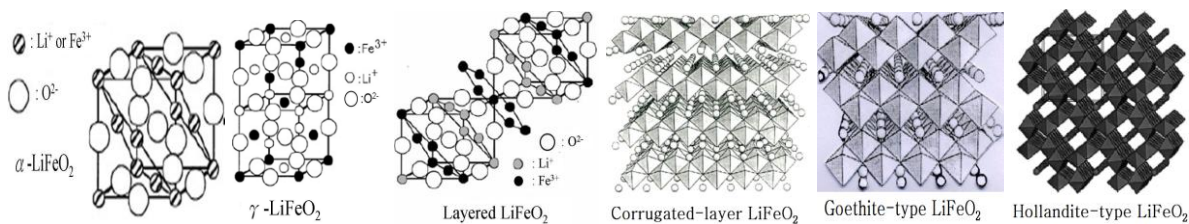


**Figure 1.** Various crystalline structures of LiFeO<sub>2</sub>

LiFeO<sub>2</sub> has various crystalline structures, as shown in Fig.1[1].  $\alpha$ -LiFeO<sub>2</sub> has cations-disordered cubic rock-salt structure with a space group of  $Fm\bar{3}m$ .  $\gamma$ -LiFeO<sub>2</sub> with a space group of  $I4_1/amd$  can be obtained by reducing the symmetry from cubic to tetragonal by ordering the Li<sup>+</sup> and Fe<sup>3+</sup> ions at octahedral sites.  $\beta$ -LiFeO<sub>2</sub> with a space group of  $C2/c$  is formed as an intermediate phase during the ordering process. Layered LiFeO<sub>2</sub> constructed with rhombohedral lattice shows similar structure with  $\alpha$ -NaFeO<sub>2</sub> rock-salt structure with a space group of  $R\bar{3}m$ . Li<sup>+</sup> and Fe<sup>3+</sup> alternatively occupy the octahedral sites produced by the O<sup>2-</sup> cubic close packed array.

Corrugated LiFeO<sub>2</sub> constructed of orthorhombic lattice with a space group of  $Pmnm$  is consisted with a ccp oxygen array and cation sheets made of alternating pairs of Li<sup>+</sup> and Fe<sup>3+</sup> rows. Goethite-type LiFeO<sub>2</sub>, having the same orthorhombic lattice and space group of  $Pbnm$  as those of  $\alpha$ -FeOOH. Hollandite-type LiFeO<sub>2</sub> has the same symmetry as the  $\beta$ -FeOOH that has tetragonal lattice and a space group of  $I4/m$ .

The crystalline structure of LiFeO<sub>2</sub> depends mainly on the preparation route. Table 1 summarizes preparation and electrochemical performance of various type of LiFeO<sub>2</sub> proposed in the literatures.

Inactive cubic rock-salt  $\alpha$ -LiFeO<sub>2</sub> will be obtained when using high-temperature solid state reaction above 600°C. Up to now, all of the reported electroactive LiFeO<sub>2</sub> including  $\alpha$ -LiFeO<sub>2</sub>[3,4,8,10], goethite-type LiFeO<sub>2</sub>[15], hollandite-type LiFeO<sub>2</sub>[21], corrugated layer LiFeO<sub>2</sub>[15,16-20] are prepared by using low-temperature synthesis technology such as ion-exchange method, hydrothermal synthesis, solvent-thermal synthesis, low-temperature solid state reaction, low-temperature molten salt method.

Based on these papers, the characteristic of electroactive LiFeO<sub>2</sub> can be summarized as follows:

1) First charge plat voltage is above 4V, corresponding to Fe<sup>4+</sup>/Fe<sup>3+</sup> couple reaction, however, large voltage hysteresis is observed during the discharge step, as shown in Fig.2. The discharge voltage decreases rapidly to 3V, and the subsequent charge-discharge mainly proceeds during voltage range of 1.5~3.5V, that leads to small capacity above 4V. Two reasons have been presented. One reason is irreversible structure change during the first charge. Sakurai et al.[8,15] pointed out that unusual Fe<sup>4+</sup> ions generated during charging may play an important role in the occurrence of voltage hysteresis.

**Table 1.** Preparation and electrochemical performance of various type of LiFeO<sub>2</sub> proposed in the literatures

Type	Structure	Preparation method	Preparation procedure	Electrochemical performance in references
$\alpha$ -LiFeO <sub>2</sub>	<i>Fm3m</i> (cubic) Cations disordered	Solid state reaction	Mixture of Li <sub>2</sub> CO <sub>3</sub> and Fe <sub>2</sub> O <sub>3</sub> annealed above 600°C	[2]
		Low-temperature molten salt synthesis	$\beta$ -FeOOH, LiNO <sub>3</sub> +LiOH molten salt (Li/Fe=4)heated at 250°C for 3h in air	~80mAh/g(5 <sup>th</sup> cycle)[3]
			$\alpha$ -FeOOH, LiNO <sub>3</sub> +LiOH molten salt (molar ratio1:2:2)heated at 250°C for 3h in air	~150 mAh/g(50 <sup>th</sup> cycle)[4]
		Hydrothermal synthesis	Synthesis of Fe(NO <sub>3</sub> ) <sub>3</sub> hydrolyzed gel with Li <sup>+</sup> sol.(6M) at 160°C for 24h	[5]
			Synthesis of LiOH sol. with $\alpha$ -FeOOH or Fe(III) sol. (Li/Fe=20~30) at 156~220°C for 5h	[6,7]
		Solvent-thermal synthesis	Synthesis of $\alpha$ -FeOOH with LiOH·H <sub>2</sub> O(Li/Fe=3~5) in 2-phenoxyethanol at 150~200°C for 4h	Initial capacity of ~80 mAh/g, ~50 mAh/g during cycling [8]
			Synthesis of FeCl <sub>3</sub> with LiOH·H <sub>2</sub> O(Li/Fe≥10) in ethanol at 280°C for 8h	[9]
Ion-exchange	Ion-exchange between $\beta$ -FeOOH and LiOH·H <sub>2</sub> O(Li/Fe=2) in ethanol at 85°C for 3h	Initial capacity of ~110 mAh/g, ~70 mAh/g during cycling [10]		
$\beta$ -LiFeO <sub>2</sub>	Structure between $\alpha$ - and $\gamma$ -LiFeO <sub>2</sub> Cations ordered	Heat treatment	$\alpha$ -LiFeO <sub>2</sub> heated at 350~400°C	[6]
		Hydrothermal synthesis	Synthesis of Fe(NO <sub>3</sub> ) <sub>3</sub> hydrolyzed gel with Li <sup>+</sup> sol.(6M) at 160°C for 336h	[5]
		Ion-exchange	Ion-exchange of $\alpha$ -NaFeO <sub>2</sub> in LiCl/KCl molten salts at 500°C	[11]
$\gamma$ -LiFeO <sub>2</sub>	<i>I4/amd</i> (tetragonal) Cations ordered	Heat treatment	$\alpha$ -LiFeO <sub>2</sub> heated at 480°C for 192h	[6]
		Hydrothermal synthesis	Synthesis of Fe(NO <sub>3</sub> ) <sub>3</sub> hydrolyzed gel with Li <sup>+</sup> sol.(6M) at 160°C for 912h	[5]
Layered LiFeO <sub>2</sub>	<i>R3m</i> (rhombohedral)	Ion-exchange	Ion-exchange of $\alpha$ -NaFeO <sub>2</sub> in low-temperature molten salts	[11,12]
			Ion-exchange of $\alpha$ -NaFeO <sub>2</sub> with LiOH·H <sub>2</sub> O in alcohol at 140°C	[13]
		Hydrothermal synthesis	Synthesis of $\alpha$ -FeOOH with LiOH+KOH sol.(excess LiOH) at 220°C for 2h	[14]
Goethite-type LiFeO <sub>2</sub>	<i>Pbmm</i> (orthorhombic)	Ion-exchange	Ion-exchange of $\alpha$ -FeOOH with C <sub>2</sub> H <sub>5</sub> OLi in ethanol at 170°C for 15h	~70 mAh/g [15]
		Solvent-thermal synthesis	Synthesis of $\alpha$ -FeOOH with LiOH·H <sub>2</sub> O(Li/Fe=1) in 2-phenoxyethanol at 150~200°C for 4h	[8]
Hollandite-type LiFeO <sub>2</sub>	<i>I4/m</i> (tetragonal)	Ion-exchange	Ion-exchange of $\beta$ -FeOOH with ROLi	~150 mAh/g[21]
Corrugated layer LiFeO <sub>2</sub>	<i>Pmnm</i> (orthorhombic)	Low-temperature molten salt synthesis	Mixture of $\gamma$ -FeOOH and LiOH·H <sub>2</sub> O heated at 150°C for 15h in Ar	Initial capacity of ~150 mAh/g, 73% retains after 50 cycles [16-18]
		Ion-exchange	Ion-exchange of $\gamma$ -FeOOH with C <sub>2</sub> H <sub>5</sub> OLi in ethanol at 140°C for 15h	~60 mAh/g [19]
			Ion-exchange of $\gamma$ -FeOOH with ROLi at 115°C for 4h	~110 mAh/g [15]
			Ion-exchange of $\gamma$ -FeOOH with LiOH·H <sub>2</sub> O(Li/Fe=1.4)at 200°C for 1~5h	Initial capacity of ~135 mAh/g, 100~110 mAh/g during cycling [20]

Kanno et al.[20] speculated that the conversion proceeds from the corrugated layer structure LiFeO<sub>2</sub> to an amorphous phase during the first charge, and charge-discharge process after the second

cycles proceeds in the amorphous phase. After investigating the structure change of nano  $\alpha$ -LiFeO<sub>2</sub> in the charge/discharge process by using XRD, Morales et al.[4] considered a structural rearrangement upon lithium removal, which was similar to the results reported for a Li<sub>4/3</sub>Ti<sub>2/3</sub>O<sub>2</sub>-LiFeO<sub>2</sub> solid solution prepared by Tabuchi et al. [42]. In this work, the authors proposed that Fe<sup>4+</sup> atoms are displaced from octahedral 4a sites to tetrahedral 8c positions, and therefore hinder lithium diffusion during charge, which accounts for the disparate profiles of the charge–discharge curves. The amount of Li inserted in the first discharge was close to 1.4Li per formula unit, indicating that an excess of Li<sup>+</sup> may be intercalated into empty tetrahedral 8c positions, which results in a pseudo-plateau close to 1.7 V.

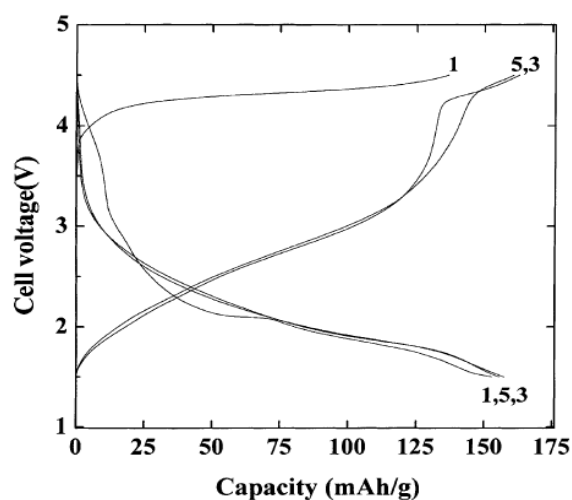


**Figure 2.** Charge/discharge curves of LiFeO<sub>2</sub> [17]

Another reason is that unstable Fe<sup>4+</sup> formed during charge may react with electrolyte. Bordet-Le. Guenne et al.[19] investigated the structure of corrugated layer LiFeO<sub>2</sub> during charge/discharge by using XRD and Mössbauer spectra analysis, and proposed that unstable Fe<sup>4+</sup> formed during charge process oxidize the electrolyte to produce Fe<sup>3+</sup> species, leading to Fe<sup>3+</sup>/Fe<sup>2+</sup> couple reaction during discharge. The charge/discharge plateaus at around 2.6 and 2.1V after initial cycle suggests that the electrochemical active of corrugated layer LiFeO<sub>2</sub> are due to the reactions of the Fe<sup>3+</sup>/Fe<sup>2+</sup> couple and the intercalation of Li<sup>+</sup> ions into the tetrahedral sites of the random. Results of in situ XANES further proved the reversible electrochemical reaction can be written as: Li<sub>1+x</sub>FeO<sub>2</sub> ↔ LiFeO<sub>2</sub> + xLi<sup>+</sup> + e<sup>-</sup>. Morales et al.[22] also confirmed that Fe<sup>2+</sup> may exist after first discharge, and the strong exothermic peak close to 398K in DSC curve may result from the reaction of Fe<sup>4+</sup> with electrolyte.

Based on above reported results, we can conclude that the oxidation extent of Fe<sup>3+</sup> to Fe<sup>4+</sup> in LiFeO<sub>2</sub> during first charge plays important role to its electrochemical performance in subsequent charge/discharge cycles.

2) Smaller particle sizes or larger specific area are beneficial to electrochemical active of LiFeO<sub>2</sub> powders. As described before, all of the reported electroactive LiFeO<sub>2</sub> including  $\alpha$ -LiFeO<sub>2</sub>[3,4,8,10], goethite-type LiFeO<sub>2</sub>[15], hollandite-type LiFeO<sub>2</sub>[21], corrugated layer

$\text{LiFeO}_2$ [15,16-20] are prepared by using low-temperature synthesis technology, which ensure preparation of nano-size  $\text{LiFeO}_2$ . In view of structure, disordered rock-salt cubic  $\alpha\text{-LiFeO}_2$  should be electrochemical inactive due to no pathway for  $\text{Li}^+$  diffusion. However, nano-sized  $\alpha\text{-LiFeO}_2$  prepared by low-temperature synthesis is electroactive. Nanorods  $\alpha\text{-LiFeO}_2$  with average diameter of 80nm and average length of 900nm has been reported by Wang et al.[3] to have reversible capacity of  $\sim 80\text{mAh/g}$ , which is higher than that of the bulk sample (ca.  $65\text{mAh/g}$ ). The improved properties were ascribed in the literature to the increased surface area of  $\alpha\text{-LiFeO}_2$  nanorods, which facilitates the deintercalation and intercalation of  $\text{Li}^+$ . Morales et al.[4] reported that the  $\alpha\text{-LiFeO}_2$  sample with about 50 nm in size and bunch-like morphology can show capacity of  $\sim 150\text{mAh/g}$ , which are much higher than the reported nanorods  $\alpha\text{-LiFeO}_2$ [3]. This paper attributed the outstanding performance to smaller size and bunch architecture of the material, which can provide a not-interrupted pathway for lithium ion diffusion. As described before, the oxidation extent of  $\text{Fe}^{3+}$  to  $\text{Fe}^{4+}$  in  $\text{LiFeO}_2$  during first charge plays important role to its electrochemical performance in subsequent charge/discharge cycles. We can speculate that smaller size and higher specific area of  $\text{LiFeO}_2$  particles can ensure more  $\text{Fe}^{4+}$  formed during the first charge, therefore leading to higher reversible capacity in subsequent charge/discharge cycles. The speculation can interpret the reason for electrochemical active of disordered rock-salt cubic nano-size  $\alpha\text{-LiFeO}_2$ .

3) Most of reported electroactive  $\text{LiFeO}_2$  materials show faster capacity fading, especially during early cycles. Current researches show that the capacity fading is related closely to the structural change during cycling. Corrugate layer  $\text{LiFeO}_2$  has been reported by Lee et al.[17,18] to exhibit initial capacity of  $\sim 150\text{mAh/g}$  and 73% capacity retention after 50 cycles. Ex-situ XRD confirmed that the layer  $\text{LiFeO}_2$  undergoes a structural change to the spinel  $\alpha\text{-}$  or  $\beta\text{-LiFe}_5\text{O}_8$  phase during the charge/discharge process which resulted in the capacity decline during the long-term cycling. Further analysis by using in-situ XRD and TEM[16] indicates that structural change occurred during first cycling, and the clear spinel  $\text{LiFe}_5\text{O}_8$  phase found in the electrode after the 3rd cycle showed no big difference compared with that of the electrode after 50 cycles. That means that the structural change into the spinel was almost complete during the first cycle, which might be the main reason to induce the abrupt capacity loss of  $\text{LiFeO}_2$  during the early stage.

### 3. $\text{LiFeO}_2\text{-LiAO}_2$ (A=Co, Ni, Mn) SOLID SOLUTION

#### 3.1. $\text{LiFeO}_2\text{-LiCoO}_2$ solid solution

Among  $\text{LiFeO}_2\text{-LiCoO}_2$  solid solution, Fe-substituted  $\text{LiCoO}_2$ , as shown  $\text{LiCo}_{1-y}\text{Fe}_y\text{O}_2$ , has been widely investigated. Alcantara et al.[23] found single phase  $\text{LiCo}_{1-y}\text{Fe}_y\text{O}_2$  products can be obtained for  $0 \leq y \leq 0.2$ . For  $y \geq 0.2$ , diffraction lines corresponding to cubic  $\alpha\text{-LiFeO}_2$  can be observed. Tabuchi et al.[24] reported that the homogeneous  $\text{LiCo}_{1-y}\text{Fe}_y\text{O}_2$  solid solution is formed up to  $y = 0.25$  by a hydrothermal reaction, which is consistent with the result reported by Alcantara[23]. The sample with  $y = 0.4$  is the mixture of 80% layered phase and 20% cubic rock salt phase. The system  $\text{LiCo}_1\text{-}$

$y\text{Fe}_y\text{O}_2$  for the whole composition range was only obtained by ion-exchange of  $\text{NaCo}_{1-y}\text{Fe}_y\text{O}_2$  in a molten eutectic mixture of  $\text{LiCl}$  and  $\text{LiNO}_3$  [25,26].

Fe substitution leads to increase of cation disorder in  $\text{LiCo}_{1-y}\text{Fe}_y\text{O}_2$ . As reported by Alcantara et al.[23], presence of 1/3 Fe in Li sites cause a poorer lithium ion diffusivity and enhanced polarization for  $\text{LiCo}_{0.9}\text{Fe}_{0.1}\text{O}_2$ , resulting in lower capacity of 80mAh/g and deteriorated cycling performance. Holzapfel et al.[25,26] also found an increasing iron disorder which reaches a value of approx. 5% of iron ions on lithium sites for  $\text{LiCo}_{0.6}\text{Fe}_{0.4}\text{O}_2$ . The capacities of the first discharge are only 70 mAh/g, 10 mAh/g for  $y=0.2, 0.4$  in  $\text{LiCo}_{1-y}\text{Fe}_y\text{O}_2$ , respectively.

However, Co substitution can improve the electrochemical performance of  $\text{LiFeO}_2$  remarkably.  $\alpha\text{-NaFeO}_2$ -type layered  $\text{LiFe}_{0.9}\text{Co}_{0.1}\text{O}_2$  obtained by ion-exchange of  $\text{NaFe}_{0.9}\text{Co}_{0.1}\text{O}_2$ , exhibits an initial capacity of 205mAh/g and stable capacity of 190mAh/g after 30 cycles [27]. In this literature, Suresh et al. speculated that the stable value of the reversible capacity obtained for the  $\text{LiFe}_{0.9}\text{Co}_{0.1}\text{O}_2$  is possibly due to the stabilization of the layered structure by Co.

### 3.2. $\text{LiFeO}_2\text{-LiNiO}_2$ solid solution

Reimers[28] and Chappel[29] used solid state reaction to prepare  $\text{LiNi}_{1-y}\text{Fe}_y\text{O}_2$ . The results showed that this solid solution is only iso-structural with hexagonal  $\text{LiNiO}_2$  in the composition range  $0 \leq y \leq 0.3$ . For  $0.3 < y < 0.6$ , phase coexistence occurs between ordered layer hexagonal phase and disordered rock-salt cubic phase. For  $y \geq 0.6$ , only disordered rock-salt cubic phase can be obtained. Kanno et al.[20] prepared  $\text{LiNi}_{1-y}\text{Fe}_y\text{O}_2$  for the whole composition range by ion-exchange of  $\text{NaNi}_{1-y}\text{Fe}_y\text{O}_2$  in a molten eutectic mixture of  $\text{LiCl/KCl}$ .

Similar to  $\text{LiCo}_{1-y}\text{Fe}_y\text{O}_2$ ,  $\text{LiNi}_{1-y}\text{Fe}_y\text{O}_2$  also shows increased cation disorder after Fe substitution, which causes an enhanced polarization and decreased capacity over 2~4.2V range[28]. Therefore, Reimers considered that the presence of Fe in any layered oxide cathode material would be detrimental to cell capacity. Kanno[20] tested the charge/discharge performance of  $\text{LiNi}_{1-y}\text{Fe}_y\text{O}_2$  over 1.5~4.2V range, and the results for  $y=0.6$  and 0.8 is similar to that reported by Reimers[28]. However for  $y \leq 0.4$ , stable capacity retention during cycling and long voltage plateau below 2V corresponding to 0.7Li per formula unit is observed. No interpretation for the phenomena was presented in the paper. Due to only about 0.3~0.4Li per formula unit were deintercalated during the first charge, we speculate that  $\text{Li}^+$  may be intercalated into empty tetrahedral 8c positions corresponding to  $\text{Ni}^{3+}/\text{Ni}^{2+}$  couple reaction, which is similar to the discharge behavior of  $\text{LiFeO}_2$ .

### 3.3. $\text{LiFeO}_2\text{-LiMnO}_2$ solid solution

In order to solve the problems of lower operating voltage and poorer electrochemical active for  $\text{LiFeO}_2$ , Lee et al.[30] studied the Mn-substituted  $\text{LiFeO}_2$  ( $\text{Mn}/(\text{Fe}+\text{Mn})=0.1\text{-}0.5$ ) materials. The solid solution materials were prepared by lower-temperature solid state reaction of  $\text{LiOH}\cdot\text{H}_2\text{O}$ ,  $\gamma\text{-FeOOH}$  and  $\gamma\text{-MnOOH}$  at  $350^\circ\text{C}$ . Increase of  $\text{LiMnO}_2$  amount in solid solution results in excellent cycling stability and enhanced capacity. 10%, 50% Mn-substituted  $\text{LiFeO}_2$  show capacity of ~75mAh/g,

~140mAh/g respectively. The enhanced capacity mainly come from the fraction above 2V, especially in 2.8V plateau voltage range, which resulted from the  $\text{Mn}^{4+}/\text{Mn}^{3+}$  couple reaction. The results indicate that Mn substitution is beneficial to enhance operating voltage, capacity and cycling stability of  $\text{LiFeO}_2$ .

### 3.4. Other $\text{LiFeO}_2$ - $\text{LiAO}_2$ type solid solution

As described before, Fe substitution in  $\text{LiNiO}_2$  or  $\text{LiCoO}_2$  deteriorates the electrochemical behavior. However, Fe and Co co-substituted  $\text{LiNiO}_2$  showed a different electrochemical performance [23,31,32]. As reported by Alcantara et al.[23], the unit cell parameters of  $\text{LiNi}_{0.9}\text{Fe}_{0.1}\text{Co}_{0.2}\text{O}_2$  are different from  $\text{LiNi}_{0.9}\text{Fe}_{0.1}\text{O}_2$  and  $\text{LiCo}_{0.9}\text{Fe}_{0.1}\text{O}_2$ . Compared with  $\text{LiNi}_{0.9}\text{Fe}_{0.1}\text{O}_2$ ,  $\text{LiNi}_{0.9}\text{Fe}_{0.1}\text{Co}_{0.2}\text{O}_2$  shows a remarkable improved electrochemical performance with a capacity of 120mAh/g at 4<sup>th</sup> cycle. Prado et al.[31,32] synthesized  $\alpha$ - $\text{NaFeO}_2$ -type layer  $\text{LiNi}_{0.7}\text{Fe}_{0.15}\text{Co}_{0.15}\text{O}_2$  by high-temperature solid state reaction of  $\text{NiO}$ ,  $\text{Fe}_2\text{O}_3$ ,  $\text{Co}_3\text{O}_4$  and  $\text{Li}_2\text{CO}_3$ . Compared with  $\text{LiNi}_{0.9}\text{Fe}_{0.1}\text{O}_2$ , Co substituted material,  $\text{LiNi}_{0.7}\text{Fe}_{0.15}\text{Co}_{0.15}\text{O}_2$ , presents enhanced cation-order, structural stability and cycling performance. The paper proposed that  $\text{Co}^{3+}$  shows opposite behavior to  $\text{Fe}^{3+}$  for cation distribution, therefore Fe and Co co-substitution will be beneficial to stable the layer structure of  $\text{LiNiO}_2$ . Further Mössbauer studies showed that nickel and iron ions in  $\text{LiNi}_{0.7}\text{Fe}_{0.15}\text{Co}_{0.15}\text{O}_2$  are simultaneously oxidized during charge, and the small cobalt ions facilitate the oxidization of iron ions. Delmas et al.[33] pointed out that larger size  $\text{Fe}^{3+}$  should be prior to oxidize compared with  $\text{Ni}^{3+}$ . Nevertheless, since iron oxidation is intrinsically difficult, both cations are oxidized simultaneously.

Park et al.[34] investigated solid solution  $0.8\text{Li}_x\text{MnO}_2\text{-}0.2\text{Li}_{1-x}\text{Fe}_{0.8}\text{Ni}_{0.2}\text{O}_2$ . Compared with  $0.8\text{Li}_x\text{MnO}_2\text{-}0.2\text{Li}_{1-x}\text{FeO}_2$ ,  $0.8\text{Li}_x\text{MnO}_2\text{-}0.2\text{Li}_{1-x}\text{Fe}_{0.8}\text{Ni}_{0.2}\text{O}_2$  shows much reduced impurity, higher initial discharge capacity of above 192 mAh/g and an excellent cycle retention rate (96%) up to 45 cycles. XPS results indicate that increased discharge capacity results from the  $\text{Ni}^{3+}/\text{Ni}^{2+}$  couple reaction during charge/discharge process.

## 4. $\text{LiFeO}_2$ - $\text{Li}_2\text{MO}_3$ SOLID SOLUTION

### 4.1. $\text{LiFeO}_2$ - $\text{Li}_2\text{MnO}_3$ solid solution

As described before, unstable  $\text{Fe}^{4+}$  in  $\text{LiFeO}_2$  formed during first charge process react with electrolyte to produce  $\text{Fe}^{3+}$  species, leading to no  $\text{Fe}^{4+}/\text{Fe}^{3+}$  couple reaction during discharge process. Therefore, Tabuchi et al.[35] tried to prepare Fe-doped  $\text{Li}_2\text{MnO}_3$  to observe the  $\text{Fe}^{4+}/\text{Fe}^{3+}$  redox behavior in stable inactive  $\text{Li}_2\text{MnO}_3$  phase over 2.5~4.3V range. They presented a three-step preparation method including coprecipitation–hydrothermal– calcinations. Fe–Mn hydroxide coprecipitates were firstly prepared, then mixed with  $\text{LiOH}$  and oxidant  $\text{KClO}_3$  to prepare  $\text{Li}_{1+x}(\text{Fe}_y\text{Mn}_{1-y})_{1-x}\text{O}_2$  precursor by hydrothermal reaction at 220~340°C. The precursors were then calcinated at 500°C to obtain  $\text{Li}_{1+x}(\text{Fe}_y\text{Mn}_{1-y})_{1-x}\text{O}_2$ . 3.1% Mn/Fe occupy Li sites in the 10% Fe-doped  $\text{Li}_2\text{MnO}_3$  sample. The capacity up to 4.3V is 35~45mAh/g for the hydrothermally obtained sample,

and ~24mAh/g for the post-annealed after hydrothermal-treatment. Although the capacity is lower, the  $\text{Fe}^{4+}/\text{Fe}^{3+}$  couple reaction (corresponding to 4.0~4.5V) during first charge/discharge process can be observed by  $^{57}\text{Fe}$  Mössbauer spectra, which indicate that  $\text{Li}_2\text{MnO}_3$  can play a stable role for  $\text{Fe}^{4+}/\text{Fe}^{3+}$  couple reaction of  $\text{LiFeO}_2$ .

Subsequently, preparation conditions of the three-step method were optimized by Tabuchi et al.[36,37]. By controlling the preparation temperature of Fe–Mn co-precipitate below room temperature ( $-10^\circ\text{C}$ ), the discharge capacity of  $\text{Li}_{1.2}\text{Fe}_{0.4}\text{Mn}_{0.4}\text{O}_2$  was improved to 85mAh/g, which is twice as large as that prepared from Fe–Mn co-precipitate at room temperature. The improvement is attained mainly by lowering the 3d metal ion content in Li layer, which can be obtained from homogeneous and reactive precursor with relatively low spinel ferrite content below RT [36]. By controlling the firing temperatures at  $500\sim 700^\circ\text{C}$ , a pure O3 phase was obtained. A small amount of spinel ferrite-like  $\text{LiFe}_5\text{O}_8$  coexist as an impurity phase for the sample that was fired at  $750^\circ\text{C}$ . With increasing the firing temperature from  $500^\circ\text{C}$  to  $700^\circ\text{C}$ , all of  $\text{Fe}^{4+}$  content, cation-order,  $\text{Li}/(\text{Fe}+\text{Mn})$  ratio in  $\text{Li}_{1.2}\text{Fe}_{0.4}\text{Mn}_{0.4}\text{O}_2$  sample were enhanced, but the specific area was decreased. The maximum initial and 10<sup>th</sup> discharge capacities were obtained at  $600\text{--}650^\circ\text{C}$  because of the balance between the development of 3d cation ordering, their primary particle size, and Li content, depending on the iron valence, which is changeable between 3+ and 4+.

Above 200mAh/g capacity can be obtained for  $\text{Li}_2\text{MnO}_3$  when charged to 4.8V, so the studies on  $\text{Li}_2\text{MnO}_3\text{--LiAO}_2$  ( $\text{A}=\text{Co}, \text{Ni}, \text{Cr}, \text{Ni}_{1/3}\text{Co}_{1/3}\text{Mn}_{1/3}$  etc.) solutions have been paid more attention in recent years. Tabuchi et al.[38,39], Kikkawa et al.[40] also investigated the effects of Fe content and heat-treatment on the structure and electrochemical performance of  $\text{Li}_{1+x}(\text{Fe}_y\text{Mn}_{1-y})_{1-x}\text{O}_2$  solution over 2.1~4.8V range. The results show that a pure monoclinic phase (C2/m) sample is obtained at low Fe content less than 20%. For  $0.3\leq y\leq 0.5$ , the prepared  $\text{Li}_{1+x}(\text{Fe}_y\text{Mn}_{1-y})_{1-x}\text{O}_2$  particle is comprised of Mn-rich nanodomains with the layered rocksalt structure and Fe-rich nanodomains with the cubic rocksalt structure featured by the cation short-range order, within a common oxygen lattice framework of the cubic close-packed structure. More monoclinic phase content and more  $\text{Li}/(\text{Fe}+\text{Mn})$  ratio leads to more initial capacity. Heat-treatment can make the hydrothermal precursors change to a sample with higher  $\text{Li}/(\text{Fe}+\text{Mn})$  ratio and monoclinic phase content (>68%). Fe contents greater than 30% in the sample contribute to decreased initial capacity, but improved charge/discharge efficiency and cycling stability due to suppression of a change from layer rock-salt phase to spinel phase. The  $0.3\leq y\leq 0.5$  samples post-annealed at  $850^\circ\text{C}$  exhibits higher capacity (>220mAh/g) and better cycling performance. Post-annealing over  $850^\circ\text{C}$  can decrease the specific area of sample, leading to remarkable reduce of capacity. In addition, the  $\text{Li}/(\text{Fe}+\text{Mn})$  ratio, monoclinic phase content and specific area also influence the discharge characteristics under high current density and below room temperature. Therefore, controlling the preparation conditions is very important to the electrochemical performance of  $\text{Li}_{1+x}(\text{Fe}_y\text{Mn}_{1-y})_{1-x}\text{O}_2$ .

#### 4.2. $\text{LiFeO}_2\text{--LiAO}_2\text{--Li}_2\text{MnO}_3$ ( $\text{A}=\text{Al}, \text{Ni}, \text{Co}$ ) solid solution

Tabuchi et al.[36] studied the effects of 5% Al-, Co-, Ni-doping on the properties of

$\text{Li}_{1.2}\text{Mn}_{0.4}\text{Fe}_{0.4}\text{O}_2$ . The doping leads to slight decrease of initial capacity, but can reduce the impedance increase and improve cycling stability. The capacity retention after 10 cycles is 77% for  $\text{Li}_{1.2}\text{Mn}_{0.4}\text{Fe}_{0.4}\text{O}_2$ , and 88%, 100.5%, 93% for 5% Al-, Co-, Ni-doped sample, respectively.

Zheng et al.[41] prepared  $\alpha\text{-NaFeO}_2$ -type layer  $\text{Li}(\text{Li}_{0.15}\text{Ni}_{0.21}\text{Fe}_{0.21}\text{Mn}_{0.45})\text{O}_2$  by the process including preparation of Ni-Fe-Mn co-precipitate, high-temperature heating the precipitates to form Ni-Fe-Mn composite oxide, then annealing the oxides with excess LiOH at 900°C for 4h in air and 600°C for 8h in  $\text{O}_2$ . After charge-discharged several cycles between 3~4.8V to change the structure,  $\text{Li}(\text{Li}_{0.15}\text{Ni}_{0.21}\text{Fe}_{0.21}\text{Mn}_{0.45})\text{O}_2$  showed a reversible capacity of 120mAh/g and no capacity fading after 50 cycles over 3~4.4V range. It is particular that 80% of the initial capacity was kept after 428 cycle charge and discharge under a current density of 2C at 55°C. When charged to 4.8V, its capacity reached 148mAh/g, but the capacity fading still remained faster under a current density of 1C and 2C at 55°C.

#### 4.3. $\text{LiFeO}_2\text{-Li}_2\text{TiO}_3$ solid solution

$\text{Li}_{(4-x)/3}\text{Ti}_{(2-2x)/3}\text{Fe}_x\text{O}_2$  ( $0.18 \leq x \leq 0.67$ ) were prepared by Tabuchi et al.[42] using coprecipitation–hydrothermal– calcinations method. The maximum reversible capacity over 2.5~4.8V range reached 153mAh/g, but larger voltage polarization (1V) and poorer cyclability were observed. Two plateaus around 3 and 4V were observed on discharging. In-situ  $^{57}\text{Fe}$  Mössbauer spectroscopy showed evidence of the  $\text{Fe}^{4+}/\text{Fe}^{3+}$  redox only around the 4V region. The origin of the 3V plateau is still unknown. Although the rock-salt cubic structure remained during charge/discharge process, moving of the transition metal ions from 4a to 8c sites and oxygen loss were observed after deintercalation.

## 5. CONCLUSION

The electrochemical properties of  $\text{LiFeO}_2$  have been improved remarkably by using low-temperature synthesis technologies. However, intrinsic unstable structure of  $\text{LiFeO}_2$  leads to lower operating voltage and no  $\text{Fe}^{4+}/\text{Fe}^{3+}$  couple reaction, which limits its use.  $\text{Fe}^{4+}/\text{Fe}^{3+}$  couple reaction can be observed in  $\text{LiFeO}_2\text{-LiCoO}_2$  and  $\text{LiFeO}_2\text{-LiNiO}_2$  solid solution, but increased cation-disorder results in deterioration of electrochemical behavior above 2V. In order to stable the layer structure of  $\text{LiFeO}_2\text{-LiAO}_2$  (A=Ni,Co), the ions which can show opposite behavior to  $\text{Fe}^{3+}$  for cation distribution should be doped. Compared with  $\text{LiFeO}_2\text{-LiAO}_2$  (A=Ni,Co),  $\text{LiFeO}_2\text{-Li}_2\text{MnO}_3$  solid solution shows more promising for stabilization of  $\text{Fe}^{4+}/\text{Fe}^{3+}$  couple reaction. Nevertheless,  $\text{LiFeO}_2$  solubility is less than 20%. For higher  $\text{LiFeO}_2$  content (30%~50%), the prepared  $\text{LiFeO}_2\text{-Li}_2\text{MnO}_3$  particle is comprised of Mn-rich nanodomains with the layered rocksalt structure and Fe-rich nanodomains with the cubic rocksalt structure featured by the cation short-range order, within a common oxygen lattice framework of the cubic close-packed structure. In addition, the electrochemical behavior of  $\text{LiFeO}_2\text{-Li}_2\text{MnO}_3$  depends on many factors such as the Li/(Fe +Mn) ratio, monoclinic phase content and specific area. Therefore, controlling the preparation conditions is very important to the electrochemical performance

of  $\text{LiFeO}_2\text{-Li}_2\text{MnO}_3$ . It is inspiring that doping of  $\text{LiFeO}_2\text{-Li}_2\text{MnO}_3$  solid solution by other cation ions such as  $\text{Al}^{3+}$ ,  $\text{Ni}^{3+}$ ,  $\text{Co}^{3+}$  etc. can further suppress the negative behavior of Fe, improve the stabilization of structure and electrochemical performance. Although its properties need to be further improved, it is without doubt that doped  $\text{LiFeO}_2\text{-Li}_2\text{MnO}_3$  solid solution will be more promising new cathode materials for Li-ion batteries. The studies on doped  $\text{LiFeO}_2\text{-Li}_2\text{MnO}_3$  solid solution need to be strengthened in future.

#### ACKNOWLEDGEMENTS

This work is supported by the State Key Project of Fundamental Research of China (the project 2007CB209705 and 2011CB935902).

#### References

1. J. Y. Lin. The preparation and characterization of nano-sized  $\alpha\text{-LiFeO}_2$ -based cathode materials. Thesis of Tatung University for degree of Master of Engineering. 2008, 08.
2. V.R. Galakhov, E.Z. Kurmaev, St. Uhlenbrock et al., Electronic structure of  $\text{LiNiO}_2$ ,  $\text{LiFeO}_2$  and  $\text{LiCrO}_2$ : X-ray photoelectron and X-ray emission study. *Solid State Communications*, 1995, 95(6):347-351.
3. X. Wang, L. Gao, F. Zhou, et al. Large-scale synthesis of  $\alpha\text{-LiFeO}_2$  nanorods by low-temperature molten salt synthesis (MSS) method. *Journal of Crystal Growth*, 2004, 265: 220–223.
4. J. Morales, J. Santos-Peña. Highly electroactive nanosized  $\alpha\text{-LiFeO}_2$ . *Electrochemistry Communications*, 2007, 9: 2116–2120.
5. C. Barriga, V. Barron, R. Gancedo, et al., Lithium ferrite formation by precipitation from Fe(III) solutions. *Journal of Solid State Chemistry*, 1988, 132-140.
6. M. Tabuchi, K. Ado, H. Sakaebe, et al., Preparation of  $\text{AFeO}_2$  (A=Li, Na) by hydrothermal method. *Solid State Ionics*, 1995, 79: 220-226.
7. M. Tabuchi, S. Tsutsui, C. Masquelier, et al., Effect of cation arrangement on the magnetic properties of lithium ferrites ( $\text{LiFeO}_2$ ): Prepared by hydrothermal reaction and post-annealing method. *Journal of Solid State Chemistry*, 1998, 140:159-167.
8. Y. Sakurai, H. Arai, J. Yamaki. Preparation of electrochemically active  $\alpha\text{-LiFeO}_2$  at low temperature. *Solid State Ionics*, 1998, 113–115: 29–34.
9. Z. Han, X. Chen, W. Zhang, et al., Ethanothermal reactions to crystalline lithium ferrites. *Materials Chemistry and Physics*, 2001, 69: 292–29.
10. S. H. Wu, H.Y. Liu. Preparation of  $\alpha\text{-LiFeO}_2$ -based cathode materials by an ionic exchange method. *Journal of Power Sources*, 2007, 174: 789–794.
11. T. Shirane, R. Kanno, Y. Kawamoto, et al., Structure and physical properties of lithium iron oxide,  $\text{LiFeO}_2$ , synthesized by ionic exchange reaction. *Solid State Ionics*, 1995, 79: 227-233.
12. B. Fuchs and S. Kemmler-Sack. Synthesis of  $\text{LiMnO}_2$  and  $\text{LiFeO}_2$  in molten Li halides. *Solid State Ionics*, 1994, 68: 279-285.
13. M. Tabuchi, C. Masquelier, T. Takeuchi, et al.,  $\text{Li}^+/\text{Na}^+$  exchange from  $\alpha\text{-NaFeO}_2$  using hydrothermal reaction. *Solid State Ionics*, 1996, 90: 129-132.
14. M. Tabuchi, K. Ado, H. Kobayashi, et al., Magnetic properties of metastable lithium iron oxides obtained by solvothermal/hydrothermal reaction. *Journal of Solid State Chemistry*, 1998, 141: 554-561.
15. Y. Sakurai, H. Arai, S. Okada, et al., Low temperature synthesis and electrochemical characteristics of  $\text{LiFeO}_2$  cathodes. *Journal of Power Sources*, 1997, 68: 711-715.

16. Y.S. Lee a, S. Sato b, M. Tabuchi, et al., Structural change and capacity loss mechanism in orthorhombic Li/LiFeO<sub>2</sub> system during cycling. *Electrochemistry Communications*, 2003, 5: 549–554.
17. Y.S. Lee, S. Sato, Y.K. Sun, et al., A new type of orthorhombic LiFeO<sub>2</sub> with advanced battery performance and its structural change during cycling. *Journal of Power Sources*, 2003, 119–121: 285–289.
18. Y. S. Lee, C. S. Yoon, Y. K. Sun, et al., Synthesis of nano-crystalline LiFeO<sub>2</sub> material with advanced battery performance. *Electrochemistry Communications*, 2002, 4: 727–731.
19. L. Bordet-Le Guenne, P. Deniard, A. Lecerf, et al., Intrinsic instability of Fe<sup>4+</sup> in electrochemically oxidized ramsdellite and orthorhombic Li<sub>1-x</sub>H<sub>x</sub>FeO<sub>2</sub>. *Journal of Materials Chemistry*, 1999, 9:1127–1134.
20. R. Kanno, T. Shirane, Y. Inaba, et al., Synthesis and electrochemical properties of lithium iron oxides with layer-related structures. *Journal of Power Sources*, 1997, 68: 145–152.
21. T. Matsumura, R. Kanno, Y. Inaba, et al., *Journal of Electrochemistry Society*. 2002, 149: A1509.
22. J. Morales, J. Santos-Peña, R. Trócoli, et al., Insights into the electrochemical activity of nanosized  $\alpha$ -LiFeO<sub>2</sub>. *Electrochimica Acta*, 2008, 53: 6366–6371.
23. R. Alcántara, J.C. Jumas, P. Lavela, et al., X-ray diffraction, <sup>57</sup>Fe Mössbauer and step potential electrochemical spectroscopy study of LiFe<sub>y</sub>Co<sub>1-y</sub>O<sub>2</sub> compounds. *Journal of Power Sources*, 1999, 81–82: 547–553.
24. M. Tabuchi, K. Ado, H. Kobayashi, et al., Preparation of LiCoO<sub>2</sub> and LiCo<sub>1-x</sub>Fe<sub>x</sub>O<sub>2</sub> using hydrothermal reactions. *Journal of Materials Chemistry*, 1999, 9: 199–204.
25. M. Holzapfel, R. Schreiner, A. Ott. Lithium-ion conductors of the system LiCo<sub>1-x</sub>Fe<sub>x</sub>O<sub>2</sub>: a first electrochemical investigation. *Electrochimica Acta*, 46 (2001) 1063–1070.
26. M. Holzapfel, R. Schreiner, A. Ott. Lithium-ion conductors of the system LiCo<sub>1-x</sub>Fe<sub>x</sub>O<sub>2</sub>, preparation and structural investigation. *Journal of Solid State Chemistry*, 2001, 156: 470–479 .
27. P. Suresh, A.K. Shukla, N. Munichandraiah. Synthesis and characterization of LiFeO<sub>2</sub> and LiFe<sub>0.9</sub>Co<sub>0.1</sub>O<sub>2</sub> as cathode materials for Li-ion cells. *Journal of Power Sources*, 2006, 159: 1395–1400.
28. J.N. Reimers, E. Rossen, C.D. Jones, et al., Structure and electrochemistry of Li<sub>x</sub>Fe<sub>y</sub>Ni<sub>1-y</sub>O<sub>2</sub>. *Solid State Ionics*, 1993, 61: 335–344.
29. E. Chappela, G. Chouteau, G. Prado, et al., Magnetic properties of LiNi<sub>1-y</sub>Fe<sub>y</sub>O<sub>2</sub>. *Solid State Ionics*, 2003, 159: 273– 278.
30. Y.S. Lee, S. Sato, Y.K. Sun, et al., Preparation of Mn-substituted LiFeO<sub>2</sub>: A solid solution of LiFeO<sub>2</sub> and Li<sub>x</sub>MnO<sub>2</sub>. *Electrochemistry Communications*, 2003, 5: 359–364.
31. G. Prado, L. Fournès, C. Delmas. Mixed cobalt and iron substituted lithium nickelate: a structural and electrochemical study. *Solid State Ionics*, 2000, 138: 19–30.
32. G. Prado, L. Fournès, C. Delmas. On the Li<sub>x</sub>Ni<sub>0.70</sub>Fe<sub>0.15</sub>Co<sub>0.15</sub>O<sub>2</sub> system: an X-ray diffraction and Mössbauer study. *Journal of Solid State Chemistry*, 2001, 159:103–112 .
33. C. Delmas, M. Ménétrier, L. Croguennec, et al., An overview of the Li(Ni,M)O<sub>2</sub> systems: syntheses, structures and properties. *Electrochimica Acta*, 1999, 45: 243–253.
34. G.J. Park, Y.S. Lee, J. Kim, et al., Synthesis and electrochemical properties of Li<sub>1-x</sub>Fe<sub>0.8</sub>Ni<sub>0.2</sub>O<sub>2</sub>–Li<sub>x</sub>MnO<sub>2</sub> (Mn/(Fe +Ni + Mn) = 0.8) material. *Journal of Power Sources*, 2007, 174: 730–734.
35. M. Tabuchi, H. Shigemura, K. Ado, et al., Preparation of lithium manganese oxides containing iron. *Journal of Power Sources*, 2001, 97-98:415-419.
36. M. Tabuchi, A. Nakashima, K. Ado, et al., The effects of preparation condition and dopant on the electrochemical property for Fe-substituted Li<sub>2</sub>MnO<sub>3</sub>. *Journal of Power Sources*, 2005, 146: 287–293.
37. M. Tabuchi, A. Nakashima, K. Ado, et al., Heat-treatment effect on phase stability, cation distribution, chemical composition, and electrochemical behavior for Fe-substituted Li<sub>2</sub>MnO<sub>3</sub>. *Chemistry of Materials*. 2005, 17: 4668–4677.

38. M. Tabuchi, Y. Nabeshima, K. Ado, et al., Material design concept for Fe-substituted  $\text{Li}_2\text{MnO}_3$ -based positive electrodes. *Journal of Power Sources*, 2007, 174: 554–559.
39. M. Tabuchi, Y. Nabeshima, T. Takeuchi, et al., Fe content effects on electrochemical properties of Fe-substituted  $\text{Li}_2\text{MnO}_3$  positive electrode material. *Journal of Power Sources*, 2010, 195: 834–844.
40. J. Kikkawa, T. Akita, M. Tabuchi, et al., Coexistence of layered and cubic rock-salt structures with a common oxygen sublattice in  $\text{Li}_{1.2}\text{Mn}_{0.4}\text{Fe}_{0.4}\text{O}_2$  particles: A transmission electron microscopy study. *Journal of Applied Physics*, 2008, 103: 104911.
41. X. Zheng, L. Cao, W. Zhu, et al., Synthesis and performance characterization of  $\text{Li}(\text{Li}_{0.15}\text{Ni}_{0.21}\text{Fe}_{0.21}\text{Mn}_{0.45})\text{O}_2$  cathode material with good high temperature cyclability. *Acta Chimica Sinica*, 2007, 65(7):571-574.
42. M. Tabuchi, A. Nakashima, H. Shigemura, et al., Fine  $\text{Li}_{(4-x)/3}\text{Ti}_{(2-2x)/3}\text{Fe}_x\text{O}_2$  ( $0.18 \leq x \leq 0.67$ ) powder with cubic rock-salt structure as a positive electrode material for rechargeable lithium batteries. *Journal of Materials Chemistry*, 2003, 13: 1747–1757.